C. R. Mecanique 346 (2018) 634–646

Contents lists available at ScienceDirect

Comptes Rendus Mecanique

www.sciencedirect.com

Computational modeling of material forming processes / Simulation numérique des procédés de mise en forme

# Comparison of stochastic and interval methods for uncertainty quantification of metal forming processes

Maarten Arnst *, Jean-Philippe Ponthot, Romain Boman

*Université de Liège, Aérospatiale et Mécanique, Quartier Polytech, 1, allée de la Découverte 9, B-4000 Liège, Belgium*

ARTICLE INFO

*Article history:*
Received 9 October 2017
Accepted 15 January 2018
Available online 21 June 2018

*Keywords:*
Metal forming
Uncertainty quantification
Stochastic methods
Interval methods
Sensitivity analysis
Parameter study

ABSTRACT

Various sources of uncertainty can arise in metal forming processes, or their numerical simulation, or both, such as uncertainty in material behavior, process conditions, and geometry. Methods from the domain of uncertainty quantification can help assess the impact of such uncertainty on metal forming processes and their numerical simulation, and they can thus help improve robustness and predictive accuracy. In this paper, we compare stochastic methods and interval methods, two classes of methods receiving broad attention in the domain of uncertainty quantification, through their application to a numerical simulation of a sheet metal forming process.



## 1. Introduction

Various sources of uncertainty can arise in metal forming processes, or their numerical simulation, or both, such as uncertainty in material behavior, uncertainty in process conditions including friction properties, and uncertainty in geometrical properties. Here, uncertainty can refer to manufacturing variability in material behavior, process conditions, and geometry, or it can refer to the imperfect representation or incomplete knowledge of these properties in a numerical simulation. The presence of such sources of uncertainty can raise the challenge of taking into account such uncertainty in the design, the control, the optimization, the maintenance, and so forth of metal forming processes, as well as in their numerical simulation.

In the domains of uncertainty quantification and computational mechanics, new methods for the analysis and management of uncertainty are under development, see, for instance, [1–12]. These developments are very rich, and two classes of new methods receiving broad attention are the stochastic methods and the interval methods. On the one hand, stochastic methods represent uncertainty by means of probability distributions, and they rely on the probability theory to determine the impact of sources of uncertainty on quantities that depend on them. On the other hand, interval methods represent uncertainty by means of intervals, and they rely on interval arithmetic, or optimization theory, or both to determine the impact of sources of uncertainty on quantities that depend on them. Around these core tasks of representing uncertainty and determining the impact of sources of uncertainty on quantities that depend on them, research in uncertainty quantification and computational mechanics builds new methods for accounting for uncertainty in design, control, optimization, maintenance, and many other engineering tasks. These new methods from the domains of uncertainty quantification and computational mechanics can be usefully applied to the analysis and management of uncertainty in metal forming processes and their numerical simulation.

* Corresponding author.
*E-mail address:* maarten.arnst@ulg.ac.be (M. Arnst).

https://doi.org/10.1016/j.crme.2018.06.007
1631-0721/

In this paper, we compare the stochastic and interval methods through their application to a numerical simulation of a sheet metal forming process. Our intent is to provide some insight into how stochastic and interval methods handle the core tasks of representing uncertainty and determining the impact of sources of uncertainty on quantities that depend on them. The integration of these core tasks in new methods for design, control, optimization, maintenance, and other engineering tasks under uncertainty is beyond the scope of this paper. Further, we note that whereas we had already applied in two previous papers [9,13] stochastic methods to a metal forming problem with uncertain material properties, we apply here stochastic and interval methods to a metal forming problem involving not only uncertain material properties but also uncertain friction and geometrical characteristics.

This paper is organized as follows. First, in Secs. 2 and 3, we provide concise overviews of the stochastic and interval methods. Then, in Sec. 4, the core of this paper, we compare them in the context of the quantification of uncertainty in a numerical simulation of a sheet metal forming process.

## 2. Stochastic methods

Let us assume that we consider a mechanical problem that lends itself well to a representation in terms of a transformation of input parameters into a quantity of interest. Specifically, let us assume that there are a finite number, say $d$, of vector-valued input parameters, which we denote by $\boldsymbol{x}^1, \ldots, \boldsymbol{x}^d$, with $\boldsymbol{x}^1 = (x_1^1, \ldots, x_{s_1}^1)$ of dimension $s_1$ up to $\boldsymbol{x}^d = (x_1^d, \ldots, x_{s_d}^d)$ of dimension $s_d$, that are transformed through a function, which we denote by $f$, into a scalar quantity of interest, which we denote by $y$:

$$y = f(\boldsymbol{x}^1, \ldots, \boldsymbol{x}^d) \tag{1}$$

please note that in these expressions, the superscripts serve to index the vector-valued input parameters. For example, in a mechanical problem involving a metal forming process, one of the vector-valued input parameters, say $\boldsymbol{x}^1$, could collect material properties, another vector-valued input parameter, say $\boldsymbol{x}^2$, could collect friction properties, another vector-valued input parameter, say $\boldsymbol{x}^3$, could collect geometrical properties, and so forth; the quantity of interest $y$ could represent a property of the deformed piece such as a magnitude of a residual stress or a displacement component at a certain location; and the function $f$ could represent how this quantity of interest depends on these vector-valued input parameters in this metal forming process or a numerical simulation of it.

Let us assume that the vector-valued input parameters are uncertain. Within this context, we discuss below some of the key concepts of how stochastic methods allow the uncertainty in the vector-valued input parameters to be represented, its impact on the quantity of interest to be determined, and a sensitivity analysis to be carried out.

We note that this section provides only a concise overview; we refer the reader to [2,4,5,7–12] and references therein for more comprehensive texts. Further, we note that although we consider for the sake of conciseness a context involving uncertain scalars and vectors, stochastic methods are not limited to uncertain scalars and vectors and can readily deal with uncertain matrices, fields, functions, operators, and other quantities.

### 2.1. Characterization of uncertainty

Stochastic methods account for sources of uncertainty in a mechanical problem by representing them by using probability distributions. As such, the application of stochastic methods typically begins with identifying suitable probability distributions for these sources of uncertainty from available information, a task called the characterization of uncertainty.

In the present context, stochastic methods entail the representation of the uncertain vector-valued input parameters by (vector-valued) random variables, which we denote by $\boldsymbol{X}^1 = (X_1^1, \ldots, X_{s_1}^1)$ up to $\boldsymbol{X}^d = (X_1^d, \ldots, X_{s_d}^d)$; please note that it is customary in the probability theory [14] to denote random variables by using uppercase letters. We denote their probability distributions by $\pi_{\boldsymbol{X}^1} = \pi_{(X_1^1, \ldots, X_{s_1}^1)}$ up to $\pi_{\boldsymbol{X}^d} = \pi_{(X_1^d, \ldots, X_{s_d}^d)}$, respectively:

$$\boldsymbol{X}^1 \sim \pi_{\boldsymbol{X}^1}, \quad \ldots \quad , \boldsymbol{X}^d \sim \pi_{\boldsymbol{X}^d} \tag{2}$$

here, with $1 \leq j \leq d$, we denote by $\boldsymbol{X}^j \sim \pi_{\boldsymbol{X}^j}$ that $\boldsymbol{X}^j$ is distributed according to $\pi_{\boldsymbol{X}^j}$, by which the probability theory understands that $\pi_{\boldsymbol{X}^j}$ is a function that assigns to any meaningful subset $\mathcal{B}^j$ of $\mathbb{R}^{s_j}$ the probability $\pi_{\boldsymbol{X}^j}(\mathcal{B}^j)$ that the value taken by $\boldsymbol{X}^j$ is in $\mathcal{B}^j$. From the mechanical point of view, if the uncertainty refers to manufacturing variability, the probability distributions $\pi_{\boldsymbol{X}^1}, \ldots, \pi_{\boldsymbol{X}^d}$ can be interpreted as describing frequencies of occurrence of values of the uncertain vector-valued input parameters; and if the uncertainty refers to an imperfect representation or incomplete knowledge, they can be interpreted as describing plausabilities of values of the uncertain vector-valued input parameters.

We assume that the partitioning of the input uncertainty into the uncertain vector-valued input parameters is such that these uncertain vector-valued input parameters are represented appropriately by mutually statistically independent random variables, by which the probability theory understands that the joint probability distribution $\pi_{(\boldsymbol{X}^1, \ldots, \boldsymbol{X}^d)}$ of $\boldsymbol{X}^1, \ldots, \boldsymbol{X}^d$ is the product of the probability distributions $\pi_{\boldsymbol{X}^1}, \ldots, \pi_{\boldsymbol{X}^d}$:

$$\pi_{(\boldsymbol{X}^1, \ldots, \boldsymbol{X}^d)} = \pi_{\boldsymbol{X}^1} \times \ldots \times \pi_{\boldsymbol{X}^d} \tag{3}$$

From the mechanical point of view, if the uncertainty refers to manufacturing variability, this assumption means that we assume the value taken by one of the uncertain vector-valued input parameters to not affect frequencies of occurrence of values of others; and, if the uncertainty refers to an imperfect representation or incomplete knowledge, it means that we assume the value taken by one of them to not affect plausabilities of values of others.

Stochastic methods typically build on methods from mathematical statistics and information theory [15] to infer suitable probability distributions from available information. In a mechanical problem, information can be available in the form of minimum and maximum values for properties of materials guaranteed by providers of these materials, data sets containing values of properties as they occurred in series productions, expert opinions on levels of uncertainty, physical or mechanical constraints, and many other possible sources of information. In the present context, the application of stochastic methods requires the inference of $\pi_{\boldsymbol{X}^1}, \ldots, \pi_{\boldsymbol{X}^d}$ from available information. The particular way in which this inference can be carried out can be expected to depend strongly on the particular type of available information, which is why we do not attempt to provide a general overview here, but we limit ourselves to providing a concrete example later in Sec. 4.

### 2.2. Propagation of uncertainty

Stochastic methods rely on the probability theory to assess the impact of sources of uncertainty on quantities that depend on them in a mechanical problem: once probability distributions are assigned to the sources of uncertainty, the probability theory is invoked to transform these probability distributions of the sources of uncertainty into the probability distribution for quantities of interest, a task called the propagation of uncertainty.

In the present context, stochastic methods entail the representation of the quantity of interest by a random variable $Y$ that is defined as the image of the random variables $\boldsymbol{X}^1, \ldots, \boldsymbol{X}^d$ under the function $f$ and whose probability distribution $\pi_Y$ is thus the image of the joint probability distribution $\pi_{(\boldsymbol{X}^1,\ldots,\boldsymbol{X}^d)}$ of the random variables $\boldsymbol{X}^1, \ldots, \boldsymbol{X}^d$ under the function $f$:

$$Y \sim \pi_Y \quad \text{with} \quad Y = f(\boldsymbol{X}^1, \ldots, \boldsymbol{X}^d) \tag{4}$$

The probability theory constructs this transformation of probability distributions as follows: $\pi_Y$ is the probability distribution that assigns to any meaningful subset $\mathcal{B}$ of $\mathbb{R}$ precisely the probability that $\pi_{(\boldsymbol{X}^1,\ldots,\boldsymbol{X}^d)}$ assigns to the subset of values of $\mathbb{R}^{s_1} \times \ldots \times \mathbb{R}^{s_d}$ that $f$ maps into values in $\mathcal{B}$:

$$\pi_Y(\mathcal{B}) = \pi_{(\boldsymbol{X}^1,\ldots,\boldsymbol{X}^d)}(\{(\boldsymbol{x}^1, \ldots, \boldsymbol{x}^d) \in \mathbb{R}^{s_1} \times \ldots \times \mathbb{R}^{s_d} : f(\boldsymbol{x}^1, \ldots, \boldsymbol{x}^d) \in \mathcal{B}\}) \tag{5}$$

From the mechanical point of view, if the uncertainty refers to manufacturing variability, $\pi_Y$ can be interpreted as describing the frequencies of occurrence of values of the quantity of interest as they arise as a consequence of the frequencies of occurrence of values of the uncertain vector-valued input parameters; and, if the probability refers to an imperfect representation or incomplete knowledge, $\pi_Y$ can be interpreted as describing the plausabilities of values of the quantity of interest as they are implied by the plausibilities of values of the uncertain vector-valued input parameters.

Insight into the impact of the uncertainty in the vector-valued input parameters on the quantity of interest can be gleaned from the statistical descriptors of $Y$. The mean, which we denote by $m_Y$, provides a nominal value:

$$m_Y = \int_{\mathbb{R}} y \, \mathrm{d}\pi_Y(y) = \int_{\mathbb{R}^{s_1}} \ldots \int_{\mathbb{R}^{s_d}} f(\boldsymbol{x}^1, \ldots, \boldsymbol{x}^d) \mathrm{d}\pi_{\boldsymbol{X}^1}(\boldsymbol{x}^1) \ldots \mathrm{d}\pi_{\boldsymbol{X}^d}(\boldsymbol{x}^d) \tag{6}$$

that is, the mean $m_Y$ is the mathematical expectation of the random variable $Y$. The variance, which we denote by $\sigma_Y^2$, provides a measure of the amount of uncertainty induced in the quantity of interest:

$$\sigma_Y^2 = \int_{\mathbb{R}} (y - m_Y)^2 \mathrm{d}\pi_Y(y) = \int_{\mathbb{R}^{s_1}} \ldots \int_{\mathbb{R}^{s_d}} \big(f(\boldsymbol{x}^1, \ldots, \boldsymbol{x}^d) - m_Y\big)^2 \mathrm{d}\pi_{\boldsymbol{X}^1}(\boldsymbol{x}^1) \ldots \mathrm{d}\pi_{\boldsymbol{X}^d}(\boldsymbol{x}^d) \tag{7}$$

that is, the variance $\sigma_Y^2$ is the mathematical expectation of the square of the deviation of the random variable $Y$ about the mean $m_Y$. And a confidence interval $[\underline{y}_\alpha, \overline{y}_\alpha]$ associated with a confidence level of $\alpha$ with $0 \leq \alpha \leq 1$, where the subscript serves to indicate the confidence level, is an interval to which $\pi_Y$ assigns a probability exceeding $\alpha$:

$$\pi_Y([\underline{y}_\alpha, \overline{y}_\alpha]) = \int_{\mathbb{R}^{s_1}} \ldots \int_{\mathbb{R}^{s_d}} 1_{[\underline{y}_\alpha, \overline{y}_\alpha]}\big(f(\boldsymbol{x}^1, \ldots, \boldsymbol{x}^d)\big) \mathrm{d}\pi_{\boldsymbol{X}^1}(\boldsymbol{x}^1) \ldots \mathrm{d}\pi_{\boldsymbol{X}^d}(\boldsymbol{x}^d) \geq \alpha \tag{8}$$

where $1_{[\underline{y}_\alpha, \overline{y}_\alpha]}$ is the indicator function such that $1_{[\underline{y}_\alpha, \overline{y}_\alpha]}(y)$ is equal to 1 if $y$ is in $[\underline{y}_\alpha, \overline{y}_\alpha]$ and equal to 0 otherwise. Here, the second equality in (6), the second equality in (7), and the equality in (8) hold because of the probability theory's "change of variables" theorem relating integrals with respect to a probability distribution to integrals with respect to an image of it.

We note that although $\pi_Y$ is defined unequivocally by stating that it is the image of $\pi_{(\boldsymbol{X}^1,\ldots,\boldsymbol{X}^d)}$ under $f$, there is in general no closed-form expression for $\pi_Y$ as a function of $\pi_{(\boldsymbol{X}^1,\ldots,\boldsymbol{X}^d)}$ and $f$; in general, numerical simulation must be relied upon to obtain an approximation to $\pi_Y$ and its statistical descriptors, as we will discuss later in this section.

### 2.3. Sensitivity analysis

Several types of stochastic sensitivity analysis can be used, such as methods involving variance analysis, methods involving differentiation, and methods involving scatter plots and regression, correlation, and elementary effect analysis [16]. Variance-based sensitivity analysis is particularly well-established. This method allows sources of uncertainty in a mechanical problem to be ranked in an order that reflects their significance in inducing uncertainty in quantities that depend on them, and it is our focus next.

In the present context, variance-based sensitivity analysis entails determining for each uncertain vector-valued input parameter a so-called significance index. To obtain the definition of these significance indices, variance-based sensitivity analysis considers for each uncertain vector-valued input parameter the least-squares-best approximation of the function $f$ with a function of only this uncertain vector-valued input parameter:

$$f^*_{\boldsymbol{X}^j} = \arg\min_{g^*_{\boldsymbol{X}^j}} \int_{\mathbb{R}^{s_1}} \dots \int_{\mathbb{R}^{s_d}} \left| f(\boldsymbol{x}^1, \dots, \boldsymbol{x}^d) - g^*_{\boldsymbol{X}^j}(\boldsymbol{x}^j) \right|^2 \mathrm{d}\pi_{\boldsymbol{X}^1}(\boldsymbol{x}^1) \dots \mathrm{d}\pi_{\boldsymbol{X}^d}(\boldsymbol{x}^d), \quad 1 \le j \le d \tag{9}$$

These least-squares-best approximations define an expansion of $f$ in terms of so-called main effects and interaction effects as follows:

$$f(\boldsymbol{x}^1, \dots, \boldsymbol{x}^d) = m_Y + \underbrace{f_{\boldsymbol{X}^1}(\boldsymbol{x}^1)}_{\substack{\text{main effect} \\ \text{of } \boldsymbol{X}^1}} + \dots + \underbrace{f_{\boldsymbol{X}^d}(\boldsymbol{x}^d)}_{\substack{\text{main effect} \\ \text{of } \boldsymbol{X}^d}} + \underbrace{f_{(\boldsymbol{X}^1, \dots, \boldsymbol{X}^d)}(\boldsymbol{x}^1, \dots, \boldsymbol{x}^d)}_{\substack{\text{interaction effect} \\ \text{of } \boldsymbol{X}^1, \dots, \boldsymbol{X}^d}} \tag{10}$$

in which $m_Y$ still denotes the mean of $Y$ as defined in (6), the main effects $f_{\boldsymbol{X}^1}, \dots, f_{\boldsymbol{X}^d}$ are obtained by substracting $m_Y$ from the least-squares-best approximations $f^*_{\boldsymbol{X}^1}, \dots, f^*_{\boldsymbol{X}^d}$, that is,

$$f_{\boldsymbol{X}^j}(\boldsymbol{x}^j) = f^*_{\boldsymbol{X}^j}(\boldsymbol{x}^j) - m_Y, \quad 1 \le j \le d \tag{11}$$

and the interaction effect $f_{(\boldsymbol{X}^1, \dots, \boldsymbol{X}^d)}$ collects the remainder. The significance indices are then obtained by first moving in the expansion in (10) the mean $m_Y$ to the left-hand side and then squaring and integrating both sides:

$$\begin{aligned} &\underbrace{\int_{\mathbb{R}^{s_1}} \dots \int_{\mathbb{R}^{s_d}} \left| f(\boldsymbol{x}^1, \dots, \boldsymbol{x}^d) - m_Y \right|^2 \mathrm{d}\pi_{\boldsymbol{X}^1}(\boldsymbol{x}^1) \dots \mathrm{d}\pi_{\boldsymbol{X}^d}(\boldsymbol{x}^d)}_{=\sigma_Y^2} \\ &= \underbrace{\int_{\mathbb{R}^{s_1}} \left| f_{\boldsymbol{X}^1}(\boldsymbol{x}^1) \right|^2 \mathrm{d}\pi_{\boldsymbol{X}^1}(\boldsymbol{x}^1)}_{=v_{\boldsymbol{X}^1}} + \dots + \underbrace{\int_{\mathbb{R}^{s_d}} \left| f_{\boldsymbol{X}^d}(\boldsymbol{x}^d) \right|^2 \mathrm{d}\pi_{\boldsymbol{X}^d}(\boldsymbol{x}^d)}_{=v_{\boldsymbol{X}^d}} \\ &\quad + \underbrace{\int_{\mathbb{R}^{s_1}} \dots \int_{\mathbb{R}^{s_d}} \left| f_{(\boldsymbol{X}^1, \dots, \boldsymbol{X}^d)}(\boldsymbol{x}^1, \dots, \boldsymbol{x}^d) \right|^2 \mathrm{d}\pi_{\boldsymbol{X}^1}(\boldsymbol{x}^1) \dots \mathrm{d}\pi_{\boldsymbol{X}^d}(\boldsymbol{x}^d)}_{=v_{(\boldsymbol{X}^1, \dots, \boldsymbol{X}^d)}} \end{aligned} \tag{12}$$

Please note that there are no double product terms since the main and interaction effects are obtained through least-squares-best approximations and are hence orthogonal functions. Thus, the expansion of the function $f$ into main and interaction effects leads to a corresponding expansion of the variance $\sigma_Y^2$ of $Y$, whose terms are precisely the significance indices of variance-based sensitivity analysis. Specifically, recalling that the variance $\sigma_Y^2$ of $Y$ provides a measure of the amount of uncertainty induced in the quantity of interest, variance-based sensitivity analysis interprets $v_{\boldsymbol{X}^j}$ with $1 \le j \le d$ as the portion of the amount of uncertainty in the quantity of interest that is explained as stemming from the $j$-th uncertain vector-valued input parameter. By ranking the significance indices $v_{\boldsymbol{X}^1}, \dots, v_{\boldsymbol{X}^d}$ by order of magnitude, the dominant uncertain vector-valued input parameters can be identified.

We note that although the definition of the significance indices involves least-squares-best approximations and a functional expansion, numerical approximations to these significance descriptors can be obtained without explicitly constructing these least-squares best approximations and this functional expansion, as we will discuss later in this section.

### 2.4. Implementation

The implementation of the characterization of uncertainty often requires optimization methods. Indeed, methods from mathematical statistics and information theory [15] often take the form of selecting parameterized candidate probability

distributions for the sources of uncertainty and then seeking to fit them to available information by optimizing their free parameters.

A reference method for the implementation of the propagation of uncertainty is the Monte Carlo method [17]. When the uncertainty quantification involves a numerical simulation of the mechanical problem, this method requires running the numerical simulation for many different values of its input parameters, which can be computationally expensive. One way of alleviating the complexity relies on surrogate modeling, see, for instance, [2,4,5] for polynomial chaos collocation and projection methods and [18] for methods involving Gaussian processes, whose construction can be justified in a context of Bayesian inference. This approach entails constructing a surrogate model that mimics the input-output relationship in the mechanical problem and using it subsequently as a substitute for runs with the numerical simulation in the Monte Carlo method; as such, the complexity can be expected to shift to the construction of the surrogate model, whose subsequent use in the Monte Carlo method can be expected to entail virtually no overhead.

The implementation of a variance-based sensitivity analysis can be based either on methods that seek to approximate the least-squares-best approximations and the functional expansion involved in the definition of the sensitivity indices [19,20] or on methods that reinterpret these least-squares-best approximations as conditional expectations to enable the significance indices to be evaluated directly by using the Monte Carlo method [21].

## 3. Interval methods

As in the previous section, let us assume that we consider a mechanical problem that lends itself well to a representation in terms of a transformation of vector-valued input parameters into a quantity of interest as in (1). And let us assume again that the vector-valued input parameters are uncertain.

Within this context, we discuss below the representation of the uncertain vector-valued input parameters by using intervals and the determination of the corresponding interval for the quantity of interest.

We note that this section provides only a concise overview; we refer the reader to [1,3,6] and references therein for more comprehensive treatments.

### 3.1. Characterization of uncertainty

Interval methods account for sources of uncertainty in a mechanical problem by representing them by ranges of possible values, that is, by intervals.

In the present context, interval methods represent the components of the uncertain vector-valued input parameters by intervals, which we denote by

$$[\underline{x}_1^1, \overline{x}_1^1], \dots, [\underline{x}_{s_1}^1, \overline{x}_{s_1}^1], \dots, [\underline{x}_1^d, \overline{x}_1^d], \dots, [\underline{x}_{s_d}^d, \overline{x}_{s_d}^d] \tag{13}$$

### 3.2. Propagation of uncertainty

In the present context, interval methods entail the representation of the quantity of interest by the so-called solution set

$$\left\{ y \in \mathbb{R} : \; y = f(\boldsymbol{x}^1, \dots, \boldsymbol{x}^d), \; x_i^j \in [\underline{x}_i^j, \overline{x}_i^j], \; 1 \le i \le s_j, \; 1 \le j \le d \right\} \tag{14}$$

that is, the set of values of the quantity of interest that are the image under the function $f$ of values of the vector-valued input parameters when their components are constrained to belong to the intervals. In practice, interest is often restricted to finding only the range of values of the quantity of interest, that is, the smallest interval that contains the solution set, if it exists:

$$[\underline{y}, \overline{y}] \quad \text{with} \quad \underline{y} = \min_{\substack{x_i^j \in [\underline{x}_i^j, \overline{x}_i^j] \\ 1 \le i \le s_j \\ 1 \le j \le d}} f(\boldsymbol{x}^1, \dots, \boldsymbol{x}^d) \quad \text{and} \quad \overline{y} = \max_{\substack{x_i^j \in [\underline{x}_i^j, \overline{x}_i^j] \\ 1 \le i \le s_j \\ 1 \le j \le d}} f(\boldsymbol{x}^1, \dots, \boldsymbol{x}^d) \tag{15}$$

Thus, the impact of the uncertainty in the vector-valued input parameters on the quantity of interest is determined by two optimization problems that provide the minimum and maximum values of the quantity of interest when the vector-valued input parameters are constrained to belong to the intervals.

### 3.3. Implementation

A reference method for the implementation of the propagation of uncertainty consists in the solution to the optimization problems in (15) by using optimization methods. When the uncertainty quantification involves a numerical simulation of the mechanical problem, this method requires running the numerical simulation for different values of its input parameters and, depending on the optimization method, the computation of gradients, Hessians, or other information. One way of alleviating the complexity relies on surrogate modeling, and, as in the case of stochastic methods, complexity can then be expected to shift to the construction of the surrogate model.

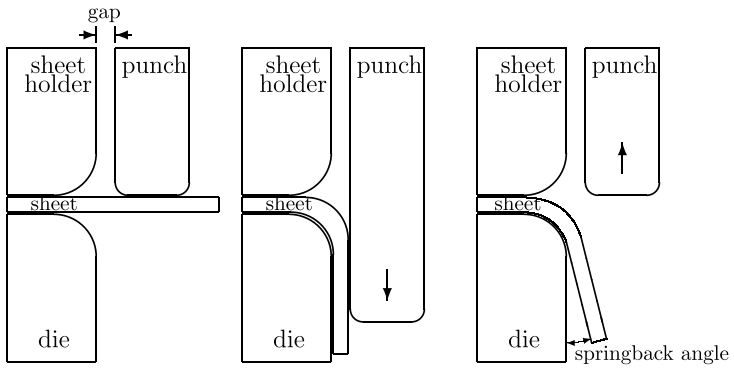


(a) Undeformed shape. (b) Imposed shape. (c) Permanently deformed shape.

**Fig. 1.** Numerical simulation and problem setting: schematic representation of the forming operation.

When the uncertainty quantification involves a numerical simulation of the mechanical problem, the propagation of uncertainty can be implemented alternatively by using interval arithmetic; however, this method is intrusive in that it requires modifications to the source code of the numerical simulation; please see [3,6] and references therein for further details.

## 4. Illustration

### 4.1. Context

In series productions of formed parts, metal forming processes are applied repeatedly to deform pieces of metal with nominally identical material behavior, under nominally identical process conditions, and with nominally identical geometrical characteristics. However, as a manifestation of manufacturing variability, even though they are nominally identical, the pieces of metal may exhibit variability in their material behavior, and the process conditions and the geometrical characteristics may exhibit variability as well; hence, each time that it is repeated, a metal forming process may yield a permanently deformed piece of metal of a different shape. In this illustration, we compare stochastic and interval methods through their application to a study of manufacturing variability in a particular forming operation.

### 4.2. Numerical simulation and problem setting

We set up in our in-house code METAFOR [22,23] a numerical simulation of a forming operation wherein a sheet is bent along a straight line (Fig. 1): a portion of the sheet is clamped and the complementary portion is bent downwards by a punch that descends until a rectangular angle is imposed, after which the punch ascends again; in such a forming operation, the sheet does not keep its rectangularly deformed shape after removing the punch; instead, it slightly springs back. We used a two-dimensional plane-strain large-displacement large-strain elastoplasticity formulation with a Krupkowski law for the hardening material behavior of the sheet and a Coulomb law for the frictional contact between the sheet and the tools. We used a penalty relaxation of the contact conditions, Enhanced Assumed Strain finite elements for the discretization of space [24], and generalized alpha time integration.

We assumed a real forming operation involved in a real series production to be accurately represented by this numerical simulation. We assumed the dominant manifestations of manufacturing variability in this real forming operation to correspond to uncertainty in the parameters $r_{\mathrm{m}}$ (ultimate yield stress) and $n$ (hardening exponent) of the Krupkowski law $\sigma_{\mathrm{y}} = k(\epsilon_0 + \epsilon_{\mathrm{p}})^n$ with $k = r_{\mathrm{m}} \exp(n)/n^n$ relating the yield stress $\sigma_{\mathrm{y}}$ to the plastic strain $\epsilon_{\mathrm{p}}$, to uncertainty in the friction coefficient $\mu$ of the Coulomb law, and to uncertainty in the size of the horizontal gap $g$ between the vertical edges of the sheet holder/die and the punch (Fig. 1) in the numerical simulation. We assumed all other characteristics to exhibit only negligible manufacturing variability in the real forming operation, and, correspondingly, we assigned fixed values to all other properties in the numerical simulation: we used a Young modulus of 210 GPa, a Poisson coefficient of 0.3, and a value of $\epsilon_0 = 5 \times 10^{-4}$ for the remaining parameter involved in the Krupkowski law; we used a value of 1 mm for the thickness of the sheet in its undeformed configuration, a shoulder radius of 3 mm, and a punch radius of 1 mm, and we assumed the sheet to be clamped along its left edge and the sheet holder to be in contact with the upper surface of the sheet in the undeformed configuration and to maintain its position; and we used a mesh whose elements are squares of size 1/6 mm $\times$ 1/6 mm in the undeformed configuration. We assumed interest to be in determining the impact of the manufacturing variability in the angle with which the sheet bends upwards again in the real forming operation, and, cor-

**Table 1**
Stochastic method: data set.

| $j$ | $(r_{\mathrm{m}j}$ [MPa], $n_j$ [−]) | $j$ | $(r_{\mathrm{m}j}$ [MPa], $n_j$ [−]) | $j$ | $(r_{\mathrm{m}j}$ [MPa], $n_j$ [−]) |
|---|---|---|---|---|---|
| 1 | (659.91, 0.1646) | 10 | (648.46, 0.1618) | 19 | (651.01, 0.1666) |
| 2 | (647.43, 0.1640) | 11 | (661.53, 0.1659) | 20 | (655.41, 0.1654) |
| 3 | (676.39, 0.1593) | 12 | (653.14, 0.1624) | 21 | (659.26, 0.1668) |
| 4 | (634.24, 0.1517) | 13 | (660.54, 0.1549) | 22 | (616.74, 0.1610) |
| 5 | (647.75, 0.1639) | 14 | (648.61, 0.1588) | 23 | (660.02, 0.1552) |
| 6 | (665.09, 0.1585) | 15 | (660.69, 0.1597) | 24 | (665.92, 0.1633) |
| 7 | (645.72, 0.1567) | 16 | (636.02, 0.1553) | 25 | (646.70, 0.1623) |
| 8 | (640.88, 0.1593) | 17 | (630.33, 0.1592) | | |
| 9 | (632.71, 0.1512) | 18 | (640.21, 0.1593) | | |

respondingly, we viewed the numerical simulation as a function $f$ that maps any value $((r_{\mathrm{m}}, n), \mu, g)$ into a corresponding value $y = f((r_{\mathrm{m}}, n), \mu, g)$ of the springback angle (Fig. 1):

$$\underbrace{y}_{\text{springback angle}} = \underbrace{f}_{\text{numerical simulation}} \Big( \underbrace{(r_{\mathrm{m}}, n)}_{\text{material}}, \underbrace{\mu}_{\text{process}}, \underbrace{g}_{\text{geometry}} \Big) \tag{16}$$

and we applied stochastic and interval methods to determine the impact of the sources of uncertainty on the springback angle.

### 4.3. Stochastic method

#### 4.3.1. Characterization of uncertainty

The application of the stochastic method entailed the representation of the uncertain ultimate yield stress and hardening exponent, the uncertain friction coefficient, and the uncertain gap by random variables, and we thus began with assigning probability distributions to them.

For the random ultimate yield stress and the hardening exponent, which we denote by $R_{\mathrm{m}}$ and $N$, respectively, we elaborated an example of the inference of the probability distribution from available information. We assumed the available information to consist of two sources. Specifically, we assumed the first source to be a data set $\{(r_{\mathrm{m}j}, n_j),\ 1 \le j \le m\}$ of $m = 25$ samples of the ultimate yield stress and the hardening exponent that occurred in the real forming operation in the series production (Table 1); such a data set could have been obtained by representatively withdrawing $m = 25$ sheets used in the real forming operation in the series production and submitting a sample taken from each one of them to a tensile test. We assumed the second source to consist of minimum and maximum values of the ultimate yield stress and the hardening exponent guaranteed by the provider of the metal used in the real forming operation in the series production: we assumed minimum and maximum values of the ultimate yield stress and of the hardening exponent of 600 MPa and 700 MPa and of 0.14 and 0.22, respectively. We obtained the probability distribution by selecting a parametrized probability density function (PDF) and fitting its parameters to the available information. Specifically, we selected the truncated bivariate gamma PDF

$$\rho_{(R_{\mathrm{m}},N)}(r_{\mathrm{m}}, n) = \underbrace{c}_{\substack{\text{normalization}\\ \text{constant}}} \times \underbrace{1_{[\underline{r}_{\mathrm{m}}, \overline{r}_{\mathrm{m}}]}(r_{\mathrm{m}}) 1_{[\underline{n}, \overline{n}]}(n)}_{\text{truncation}} \times \underbrace{\rho_{\Gamma_1\Gamma_2}(r_{\mathrm{m}}, n; \alpha_1, \beta_1, \alpha_2, \beta_2, \rho)}_{\text{bivariate gamma PDF [25]}} \tag{17}$$

To clarify the link with the notion of probability distribution that we used in Sec. 2, please note that, within the probability theory, the PDF $\rho_{(R_{\mathrm{m}},N)}$ is a representation of the probability distribution $\pi_{(R_{\mathrm{m}},N)}$ that assigns to any meaningful subset $\mathcal{B}$ of values of the ultimate yield stress and the hardening exponent the probability $\pi_{(R_{\mathrm{m}},N)}(\mathcal{B}) = \iint_{\mathcal{B}} \rho_{(R_{\mathrm{m}},N)}(r_{\mathrm{m}}, n)\, \mathrm{d}r_{\mathrm{m}}\, \mathrm{d}n$. We took into account the data set by fitting to it the parameters $\alpha_1$, $\beta_1$, $\alpha_2$, $\beta_2$, and $\rho$ of the bivariate gamma PDF, whose expression can be found in [25]. We used the method of maximum likelihood, a popular data-fitting method from mathematical statistics, which led to the optimization problem

$$(\alpha_1, \beta_1, \alpha_2, \beta_2, \rho) = \arg \max_{\substack{\tilde{\alpha}_1, \tilde{\beta}_1, \tilde{\alpha}_2, \tilde{\beta}_2 > 0 \\ -1 < \tilde{\rho} < 1}} \prod_{j=1}^{m} \underbrace{\rho_{\Gamma_1\Gamma_2}(r_{\mathrm{m}j}, n_j; \tilde{\alpha}_1, \tilde{\beta}_1, \tilde{\alpha}_2, \tilde{\beta}_2, \tilde{\rho})}_{\substack{\text{likelihood of parameter values } \tilde{\alpha}_1, \tilde{\beta}_1,\\ \tilde{\alpha}_2, \tilde{\beta}_2, \text{ and } \tilde{\rho} \text{ given data point } (r_{\mathrm{m}j}, n_j)}} \tag{18}$$

as a solution to which we obtained the shape parameters $\alpha_1 = 2346$ and $\alpha_2 = 1330$, the scale parameters $\beta_1 = 0.2770$ MPa and $\beta_2 = 1.205 \times 10^{-4}$, and the correlation coefficient $\rho = 0.3408$. And we took into account the minimum and maximum values of the ultimate yield stress and the hardening exponent by setting $[\underline{r}_{\mathrm{m}}, \overline{r}_{\mathrm{m}}] = [600, 700]$ MPa and $[\underline{n}, \overline{n}] = [0.14, 0.22]$. Fig. 2 shows a contour plot of the PDF thus obtained, which highlights a good fit with the data set and consistency with the minimum and maximum values of the ultimate yield stress and the hardening exponent.

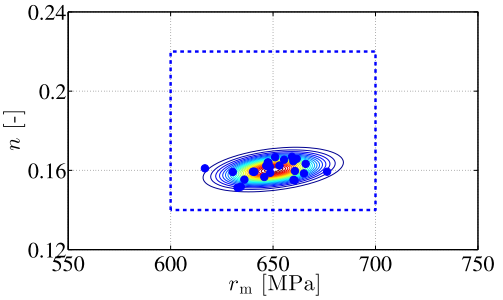


**Fig. 2.** Stochastic method: contour plot of PDF assigned to the random ultimate yield stress and the hardening exponent (solid lines), data set (dots), and minimum and maximum values of the ultimate yield stress and the hardening exponent (dashed lines).

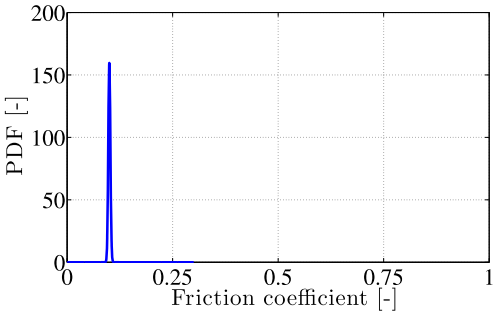


**Fig. 3.** Stochastic method: PDF assigned to the random friction coefficient.

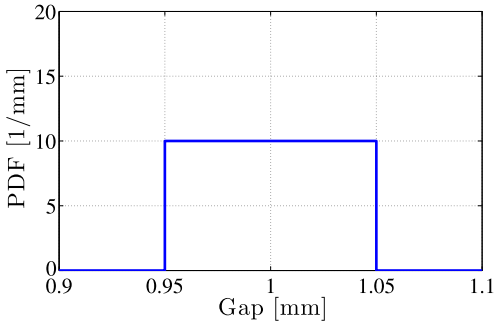


**Fig. 4.** Stochastic method: PDF assigned to the random gap.

To the random friction coefficient, denoted by $M$, we assigned a truncated beta probability distribution with PDF

$$\rho_M(\mu) = \underbrace{c}_{\substack{\text{normalization}\\ \text{constant}}} \times \underbrace{1_{[\underline{\mu},\overline{\mu}]}(\mu)}_{\text{truncation}} \times \underbrace{\rho_B(\mu;\alpha,\beta)}_{\text{beta PDF}} \tag{19}$$

with $[\underline{\mu},\overline{\mu}] = [0, 0.3]$, $\alpha = 1440$, and $\beta = 12960$ (Fig. 3), and to the random gap, denoted by $G$, we assigned a uniform probability distribution with PDF

$$\rho_G(g) = \underbrace{c}_{\substack{\text{normalization}\\ \text{constant}}} \times 1_{[\underline{g},\overline{g}]}(g) \tag{20}$$

with $[\underline{g},\overline{g}] = [0.95, 1.05]$ mm (Fig. 4). We note that the constant $c$ denotes the normalization constant in (17), (19), and (20) but has a different value in each one of these equations. The value $\underline{\mu} = 0$ can be interpreted as ideally lubricated contact between the sheet and the tools, the value $\overline{\mu} = 0.3$ can be interpreted as very dry frictional contact between the sheet and the tools, and the values of the gap contained between 0.95 mm and 1.00 mm correspond to values for which the gap is narrower than the thickness of the sheet, thus requiring thinning of the sheet. Other than these interpretations, the assignment of these probability distributions is rather arbitrary; we could have elaborated examples to show how they could have been inferred from available information, but we did not do so for the sake of brevity.

Thus, the characterization of uncertainty led to the PDFs $\rho_{(R_{\mathrm{m}},N)}$, $\rho_M$, and $\rho_G$ that serve in the stochastic method as descriptions of the frequencies of occurrence of values of the variable properties of the material behavior, the process conditions, and the geometry in the real forming operation.

*4.3.2. Surrogate model*

Next, we built a surrogate model to serve as a substitute for the numerical simulation in the propagation of uncertainty and the sensitivity analysis.

We used the nonintrusive stochastic projection method [4,5,9,11,12]. Our application of this method led us to begin with defining a grid of combinations of values of the ultimate yield stress and the hardening exponent, the friction coefficient, and the gap $\{((r_{\mathrm{m}i}, n_j), \mu_k, g_\ell),\ 1 \leq i, j, k, \ell \leq r\}$, in which $r_{\mathrm{m}i} = (\overline{r}_{\mathrm{m}} + \underline{r}_{\mathrm{m}})/2 + \xi_i(\overline{r}_{\mathrm{m}} - \underline{r}_{\mathrm{m}})/2$, $n_j = (\overline{n} + \underline{n})/2 + \xi_j(\overline{n} - \underline{n})/2$, $\mu_k = (\overline{\mu} + \underline{\mu})/2 + \xi_k(\overline{\mu} - \underline{\mu})/2$, and $g_\ell = (\overline{g} + \underline{g})/2 + \xi_\ell(\overline{g} - \underline{g})/2$, with $\xi_1, \ldots, \xi_r$ the nodes of the $r$-node Gauss–Legendre quadrature rule when the domain of integration is taken as $[-1, 1]$. Then, we ran the numerical simulation for each one of these combinations of values to obtain the corresponding values of the springback angle $\{y_{ijk\ell} = f((r_{\mathrm{m}i}, n_j), \mu_k, g_\ell),\ 1 \leq i, j, k, \ell \leq r\}$. Finally, we solved a least-squares optimization problem to fit to the training data thus obtained a surrogate model in the form of a multivariate polynomial $y = f^p((r_{\mathrm{m}}, n), \mu, g) = \sum_{\alpha+\beta+\gamma+\delta=0}^{p} c_{\alpha\beta\gamma\delta}\, r_{\mathrm{m}}^{\alpha}\, n^{\beta}\, \mu^{\gamma}\, g^{\delta}$; we note that in

$$y = \underbrace{f^p}_{\text{surrogate model}}\big((r_{\mathrm{m}}, n), \mu, g\big) \tag{21}$$

the superscript $p$ is not an exponent but serves to distinguish the surrogate model from the numerical simulation, as well as to emphasize its truncation at a polynomial degree of $p$; for the well-posedness of the least-squares optimization problem, the value of $p$ must be selected such that $p < r$.

We obtained all results to follow with $r = 5$ and $p = 3$; for $r = 5$, we had to run the numerical simulation $625 = 5^4$ times. These values are a compromise between the computational cost of the runs of the numerical simulation and the accuracy of the surrogate model; at the expense of a higher computational cost entailed by an increased number of runs of the numerical simulation, accuracy can be improved by increasing $r$ and $p$.

We used the surrogate model to gain some insight into the dependence of the springback angle on the ultimate yield stress and the hardening exponent, the friction coefficient, and the gap (Fig. 5). We can observe that the dependence on the ultimate yield stress and the hardening exponent is fairly linear and that the dependence on the friction coefficient and the gap is more nonlinear. Further, we can observe that the springback angle depends most significantly on the gap, especially for values of the gap between 0.95 mm and 1.00 mm, thus suggesting that the springback angle is significantly influenced by the thinning that the sheet must undergo for these values of the gap.

*4.3.3. Propagation of uncertainty*

Subsequently, the stochastic method entailed the representation of the springback angle by a random variable $Y$ that is defined as the image of the random ultimate yield stress and the hardening exponent $(R_{\mathrm{m}}, N)$, the random friction coefficient $M$, and the random gap $G$ under the numerical simulation $f$. We applied the Monte Carlo method to obtain an approximation to the PDF of the random springback angle and statistical descriptors of it, whereby we used the surrogate model $f^p$ as a substitute for the numerical simulation $f$. We thus began with using random number generation methods [17] to generate independent sets of $\nu$ independent samples from the PDFs $\rho_{(R_{\mathrm{m}},N)}$, $\rho_M$, and $\rho_G$, which we denote as follows:

$$\{(r_{\mathrm{m}\ell}, n_\ell),\ 1 \leq \ell \leq \nu\}, \quad \{\mu_\ell,\ 1 \leq \ell \leq \nu\}, \quad \{g_\ell,\ 1 \leq \ell \leq \nu\} \tag{22}$$

Then, we used the surrogate model to map each combination of samples into a corresponding sample of the random springback angle,

$$y_\ell^p = f^p\big((r_{\mathrm{m}\ell}, n_\ell), \mu_\ell, g_\ell\big), \quad 1 \leq \ell \leq \nu \tag{23}$$

to obtain the corresponding set of independent samples of the random springback angle, which we denote as follows:

$$\{y_\ell^p,\ 1 \leq \ell \leq \nu\} \tag{24}$$

Finally, we applied methods from mathematical statistics to deduce approximations to the PDF of the random springback angle and statistical descriptors of it. We applied the kernel density estimation method to obtain the approximation to the PDF, we applied the usual estimation methods to obtain approximations to the mean and the variance, and we determined an approximation to a confidence interval associated with a confidence level of 95% by seeking an interval that contains 95% of the samples:

$$m_Y^{p,\nu} = \frac{1}{\nu}\sum_{\ell=1}^{\nu} y_\ell^p, \qquad (\sigma_Y^{p,\nu})^2 = \frac{1}{\nu}\sum_{\ell=1}^{\nu}(y_\ell^p - m_Y^{p,\nu})^2, \qquad \frac{1}{\nu}\sum_{\ell=1}^{\nu} 1_{[\underline{y}_{95\%}^{p,\nu}, \overline{y}_{95\%}^{p,\nu}]}(y_\ell^p) \geq 95\% \tag{25}$$

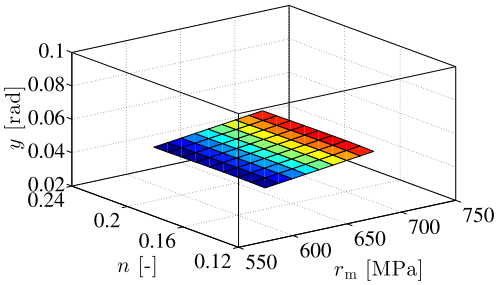


(a) $(r_{\mathrm{m}}, n) \mapsto y = f^p\big((r_{\mathrm{m}}, n), (\overline{\mu} + \underline{\mu})/2, (\overline{g} + \underline{g})/2\big)$.

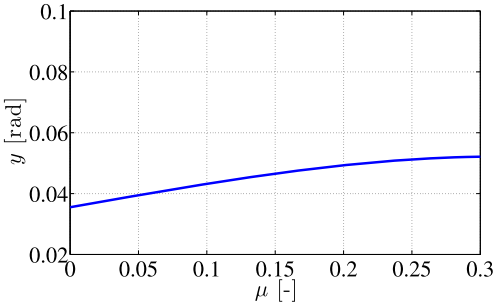


(b) $\mu \mapsto y = f^p\big(((\overline{r}_{\mathrm{m}} + \underline{r}_{\mathrm{m}})/2, (\overline{n} + \underline{n})/2), \mu, (\overline{g} + \underline{g})/2\big)$.

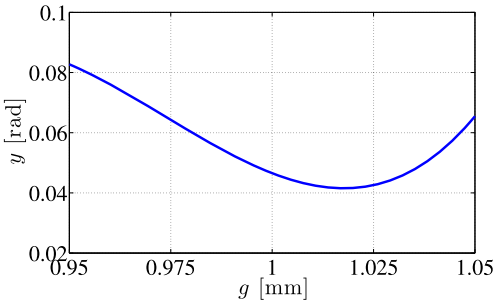


(c) $g \mapsto y = f^p\big(((\overline{r}_{\mathrm{m}} + \underline{r}_{\mathrm{m}})/2, (\overline{n} + \underline{n})/2), (\overline{\mu} + \underline{\mu})/2, g\big)$.

**Fig. 5.** Stochastic method: use of the surrogate model to gain insight into the dependence of the springback angle on the ultimate yield stress and the hardening exponent, friction coefficient, and the gap.

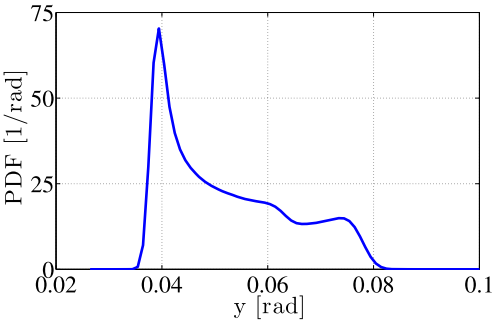


**Fig. 6.** Stochastic method: PDF of the random springback angle.

The superscripts $p$ and $\nu$ serve to indicate the use of the surrogate model as a substitute for the numerical simulation and the approximation entailed by the use of only $\nu$ samples in the Monte Carlo method, respectively.

We obtained all results to follow with $\nu = 10^6$ samples. We chose to use $\nu = 10^6$ samples by repeating the application of the Monte Carlo method for increasing values of $\nu$ and monitoring the convergence of the results.

We obtained for the random springback angle the PDF shown in Fig. 6. It is predominantly the dependence of the springback angle on the gap (Fig. 5(c)) that explains the peak in the vicinity of 0.04 rad (Fig. 6): the rather flat dependence

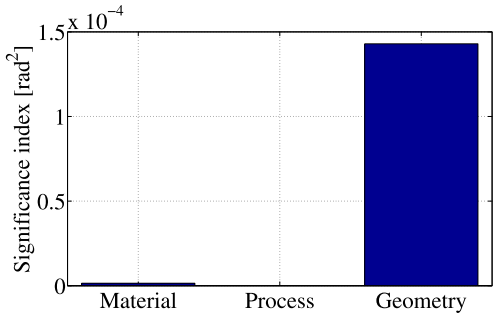


**Fig. 7.** Stochastic method: significance of uncertainty in material behavior ($\nu^{p,\nu}_{(R_{\mathrm{M}},N)}$), uncertainty in process conditions ($\nu^{p,\nu}_{M}$), and uncertainty in geometry ($\nu^{p,\nu}_{G}$) in inducing uncertainty in the springback angle.

of the springback angle on the gap for values between about 1 mm and 1.025 mm results in combinations of values of the ultimate yield stress and the hardening exponent, the friction coefficient, and the gap being mapped with significant probability into values of the springback angle in the vicinity of 0.04 rad. Further, we obtained a mean value of $m^{p,\nu}_{Y} = 0.0522$ rad, a variance of $(\sigma^{p,\nu}_{Y})^2 = 1.4439 \times 10^{-4}$ rad$^2$, and a 95%-confidence interval of $[\underline{y}^{p,\nu}_{95\%}, \overline{y}^{p,\nu}_{95\%}] = [0.0378, 0.0766]$ rad.

Thus, the propagation of uncertainty led to a PDF for the random springback angle that serves in the stochastic method as a prediction for the frequencies of springback angle value occurrences implied by the frequencies of value occurrences of the variable properties of the material behavior, the process conditions, and the geometry in the real forming operation.

#### *4.3.4. Sensitivity analysis*

Finally, we carried out a variance-based sensitivity analysis to rank the sources of uncertainty in order of significance.

We based our implementation on the method that enables the significance indices to be evaluated directly by using the Monte Carlo method [21], a method that we had already mentioned in Sec. 2.4. To obtain an approximation $\nu^{p,\nu}_{(R_{\mathrm{M}},N)}$ to the significance index $\nu_{(R_{\mathrm{M}},N)}$, our application of this method entailed the generation of one set $\{(r_{\mathrm{m}\ell}, n_\ell),\ 1 \le \ell \le \nu\}$ of $\nu$ independent samples from the PDF $\rho_{(R_{\mathrm{m}},N)}$, two independent sets $\{\mu_\ell,\ 1 \le \ell \le \nu\}$ and $\{\tilde{\mu}_\ell,\ 1 \le \ell \le \nu\}$ of $\nu$ independent samples from the PDF $\rho_M$, and two independent sets $\{g_\ell,\ 1 \le \ell \le \nu\}$ and $\{\tilde{g}_\ell,\ 1 \le \ell \le \nu\}$ of $\nu$ independent samples from the PDF $\rho_G$, followed by the computation of $\nu^{p,\nu}_{(R_{\mathrm{M}},N)}$ as $\nu^{p,\nu}_{(R_{\mathrm{M}},N)} = \frac{1}{\nu}\sum_{\ell=1}^{\nu} f^p((r_{\mathrm{m}\ell}, n_\ell), \mu_\ell, g_\ell) f^p((r_{\mathrm{m}\ell}, n_\ell), \tilde{\mu}_\ell, \tilde{g}_\ell) - (\frac{1}{\nu}\sum_{\ell=1}^{\nu} f^p((r_{\mathrm{m}\ell}, n_\ell), \mu_\ell, g_\ell))(\frac{1}{\nu}\sum_{\ell=1}^{\nu} f^p((r_{\mathrm{m}\ell}, n_\ell), \tilde{\mu}_\ell, \tilde{g}_\ell))$; to obtain $\nu^{p,\nu}_{M}$ and $\nu^{p,\nu}_{H}$, we proceeded analogously.

We obtained the values $\nu^{p,\nu}_{(R_{\mathrm{M}},N)} = 1.4654 \times 10^{-6}$ rad$^2$, $\nu^{p,\nu}_{M} = 1.3220 \times 10^{-7}$ rad$^2$, and $\nu^{p,\nu}_{G} = 1.4296 \times 10^{-4}$ rad$^2$, which correspond to $\nu^{p,\nu}_{(R_{\mathrm{M}},N)}/(\sigma^{p,\nu}_{Y})^2 = 1.01\%$, $\nu^{p,\nu}_{M}/(\sigma^{p,\nu}_{Y})^2 = 0.01\%$, and $\nu^{p,\nu}_{G}/(\sigma^{p,\nu}_{Y})^2 = 99.01\%$ (Fig. 7).

Thus, the sensitivity analysis indicates that the amount of uncertainty in the springback angle stems predominantly from the uncertainty in the gap, followed by the uncertainty in the ultimate yield stress and the hardening exponent, and lastly the uncertainty in the friction coefficient, thus suggesting that in the real forming operation, efforts to reduce the variability in the springback angle should focus on reducing the variability in the gap.

#### *4.3.5. Implementation details and computational cost*

We implemented the stochastic method in Matlab, with use of the statistics toolbox for random number generation and kernel density estimation.

The construction of the surrogate model required 625 runs of METAFOR with a total computational cost of about 20 single-core CPU hours. Because the surrogate model was cheap to evaluate, the computational cost of the rest of the stochastic method was less than 2 minutes on a single CPU core.

### *4.4. Interval method*

#### *4.4.1. Characterization of uncertainty*

We represented the uncertain ultimate yield stress and the hardening exponent by the intervals $[\underline{r}_{\mathrm{m}}, \overline{r}_{\mathrm{m}}] = [600, 700]$ MPa and $[\underline{n}, \overline{n}] = [0.14, 0.22]$, the uncertain friction coefficient by the interval $[\underline{\mu}, \overline{\mu}] = [0, 0.3]$, and the uncertain gap by the interval $[\underline{g}, \overline{g}] = [0.95, 1.05]$ mm. The bounds of these intervals are precisely the minimum and maximum values used in the preceding application of the stochastic method. Interval methods lend themselves less well to taking into account a data set such as the one that was part of the available information in the preceding application of the stochastic method.

Thus, the characterization of uncertainty led to the intervals $[\underline{r}_{\mathrm{m}}, \overline{r}_{\mathrm{m}}]$, $[\underline{n}, \overline{n}]$, $[\underline{\mu}, \overline{\mu}]$, and $[\underline{g}, \overline{g}]$ that serve in the interval method as descriptions of the ranges of values of the variable properties of the material behavior, the process conditions, and the geometry in the real forming operation.

#### *4.4.2. Surrogate model*

We reused the surrogate model that we had already built in the application of the stochastic method.

*4.4.3. Propagation of uncertainty*

We determined an approximation to the induced interval for the springback angle by solving the optimization problems $\underline{y}^p = \min f^p((r_\mathrm{m}, n), \mu, g)$ and $\overline{y}^p = \max f^p((r_\mathrm{m}, n), \mu, g)$ under the constraints that $r_\mathrm{m}$, $n$, $\mu$, and $g$ belong to the intervals $[\underline{r}_\mathrm{m}, \overline{r}_\mathrm{m}]$, $[\underline{n}, \overline{n}]$, $[\underline{\mu}, \overline{\mu}]$, and $[\underline{g}, \overline{g}]$, respectively, whereby the superscript $p$ serves to indicate that we used the surrogate model as a substitute for the numerical simulation in the optimization.

We obtained the values $[\underline{y}^p, \overline{y}^p] = [0.0264, 0.1011]$ rad; it should be noted that this interval obtained here in the application of the interval method is wider than the 95%-confidence interval $[\underline{y}^{p,\nu}_{95\%}, \overline{y}^{p,\nu}_{95\%}] = [0.0378, 0.0766]$ rad obtained previously in the application of the stochastic method.

Thus, the propagation of uncertainty led to an interval for the springback angle that serves in the interval method as a prediction for the range of values that the springback angle may take as a consequence of the ranges of values of the variable properties of the material behavior, the process conditions, and the geometry in the real forming operation.

*4.4.4. Implementation details and computational cost*

We implemented the interval method in Matlab, with use of the optimization toolbox to solve the two optimization problems. Specifically, for each one of the two optimization problems, we carried out a global search followed by a local search. The global search consisted in first using random number generation methods to generate a very large number of $10^6$ combinations of values of the ultimate yield stress, the hardening exponent, the friction coefficient, and the gap in the intervals, then using the surrogate model to evaluate the corresponding values of the springback angle, and finally identifying that combination of values at which either the minimum or the maximum value of the springback angle was attained. The local search consisted in using the combination of values thus obtained as the initial guess in a local optimization method, whereby we used the active-set method provided by the Matlab function fmincon and whereby we again used the surrogate model as a substitute for the numerical simulation. It should be noted that accuracy could be improved by using in the local search the numerical simulation itself instead of the surrogate model, but we did not do so in this work.

We reused the surrogate model whose construction had required 625 runs of METAFOR with a total computational cost of about 20 single-core CPU hours. As in the case of the application of the stochastic method, because the surrogate model was cheap to evaluate, the computational cost of the rest of the interval method beyond the construction of the surrogate model was very low, and it amounted to less than 1 minute on a single CPU core.

## 5. Conclusion

We compared stochastic methods and interval methods through their application to a numerical simulation of a sheet metal forming process:

- Both stochastic and interval methods are able to account for uncertainty in material behavior, uncertainty in process conditions including friction properties, and uncertainty in geometrical properties. However, they describe such sources of uncertainty by using different types of representation that call for different types of information to be available to be accurately defined: stochastic methods use probability distributions that represent frequencies of occurrence or degrees of plausibility, and interval methods use intervals that represent ranges of values.
- Both stochastic and interval methods are able to provide insight into the impact that sources of uncertainty can have on quantities that depend on them in a metal forming process or a numerical simulation of it, even when this dependence exhibits significant nonlinearity. However, they provide different types of insight in a manner that is consistent with their different way of representing sources of uncertainty.
- Within the context of stochastic methods, there exists a well-established type of sensitivity analysis that allows sources of uncertainty to be ranked in order of significance and dominant ones to be identified.
- When the implementation of stochastic or interval methods is built around the construction of a surrogate model, the computational cost can be expected to be dominated by the construction of this surrogate model, and when the surrogate model is cheap to evaluate, the rest of the implementation can be expected to entail only little overhead.

This paper was focused on the representation of uncertainty and the determination of the impact of sources of uncertainty on quantities that depend on them. Future work could investigate the integration of stochastic and interval methods in new methods for accounting for uncertainty in design, control, optimization, and maintenance of metal forming processes.

## References

[1] Y. Ben-Haim, I. Elishakoff, Convex Models of Uncertainty in Applied Mechanics, Elsevier, Amsterdam, The Netherlands, 1990.
[2] R. Ghanem, P. Spanos, Stochastic Finite Elements: A Spectral Approach, Dover Publications, 2003.
[3] D. Moens, D. Vandepitte, A survey of non-probabilistic uncertainty treatment in finite element analysis, Comput. Methods Appl. Mech. Eng. 194 (2005) 1527–1555.
[4] O. Le Maître, O. Knio, Spectral Methods for Uncertainty Quantification: With Applications to Computational Fluid Dynamics, Springer, 2010.
[5] D. Xiu, Numerical Methods for Stochastic Computations: A Spectral Method Approach, Princeton University Press, 2010.
[6] D. Moens, M. Hanss, Non-probabilistic finite element analysis for parametric uncertainty treatment in applied mechanics: recent advances, Finite Elem. Anal. Des. 47 (2011) 4–16, https://doi.org/10.1016/j.finel.2010.07.010.

[7] M. Grigoriu, Stochastic Systems: Uncertainty Quantification and Propagation, Springer-Verlag, 2012.
[8] R. Smith, Uncertainty Quantification: Theory, Implementation, and Applications, SIAM, 2013.
[9] M. Arnst, J.-P. Ponthot, An overview of nonintrusive characterization, propagation, and sensitivity analysis of uncertainties in computational mechanics, Int. J. Uncertain. Quantificat. 4 (2014) 387–421.
[10] T. Sullivan, Introduction to Uncertainty Quantification, Springer, 2015.
[11] R. Ghanem, D. Higdon, H. Owhadi, Handbook of Uncertainty Quantification, Springer, 2017.
[12] C. Soize, Uncertainty Quantification, Springer, 2017.
[13] M. Arnst, B. Abello Àlvarez, J. Ponthot, R. Boman, Itô-SDE MCMC method for Bayesian characterization of errors associated with data limitations in stochastic expansion methods for uncertainty quantification, J. Comput. Phys. 349 (2017) 59–79.
[14] R. Dudley, Real Analysis and Probability, Cambridge University Press, Cambridge, United Kingdom, 2002.
[15] G. Casella, R. Berger, Statistical Inference, Duxbury, Pacific Grove, California, 2002.
[16] A. Saltelli, M. Ratto, T. Andres, F. Campolongo, J. Cariboni, D. Gatelli, M. Saisana, S. Tarantola, Global Sensitivity Analysis: The Primer, Wiley, West Sussex, United Kingdom, 2008.
[17] C. Robert, G. Casella, Monte Carlo Statistical Methods, Springer, New York, 2010.
[18] C. Rasmussen, C. Williams, Gaussian Processes for Machine Learning, The MIT Press, 2006.
[19] B. Sudret, Global sensitivity analysis using polynomial chaos expansions, Reliab. Eng. Syst. Saf. 93 (2008) 964–979, https://doi.org/10.1016/j.ress.2007.04.002.
[20] T. Crestaux, O. Le Maître, J.-M. Martinez, Polynomial chaos expansion for sensitivity analysis, Reliab. Eng. Syst. Saf. 94 (2009) 1161–1172, https://doi.org/10.1016/j.ress.2008.10.008.
[21] I. Sobol, Global sensitivity indices for nonlinear mathematical models and their Monte Carlo estimates, Math. Comput. Simul. 55 (2001) 271–280, https://doi.org/10.1016/S0378-4754(00)00270-6.
[22] J. Ponthot, Traitement unifié de la mécanique des milieux continus solides en grandes deformations par la méthode des éléments finis, Ph.D. thesis, University of Liège, Liège, Belgium, 1995.
[23] Metafor, website, http://metafor.ltas.ulg.ac.be/.
[24] Q. Bui, L. Papeleux, J. Ponthot, Numerical simulation of springback using enhanced assumed strain elements, Finite Elem. Anal. Des. 153–154 (2004) 314–318, https://doi.org/10.1016/j.jmatprotec.2004.04.342.
[25] P. Moran, Statistical inference with bivariate gamma distributions, Biometrika 56 (1969) 627–634, http://www.jstor.org/stable/2334670.